Chemical Engineering Journal 151 (2009) 97–104

Contents lists available at ScienceDirect

Chemical Engineering Journal

journal homepage: www.elsevier.com/locate/cej

Decolorization and COD reduction of paper industrial effluent using electro-coagulation

K.S. Parama Kalyani [a], N. Balasubramanian [a,*], C. Srinivasakannan [b]

[a] Department of Chemical Engineering, A.C. Tech Campus, Anna University, Chennai 600 025, India
[b] School of Engineering, Monash University, Sunway Campus, Malaysia

ARTICLE INFO

Article history:
Received 4 September 2008
Received in revised form 8 December 2008
Accepted 30 January 2009

Keywords:
Pulp and paper effluent
COD reduction
Biodegradability index
Color removal
Adsorption isotherm
Reaction kinetics

ABSTRACT

Electro-coagulation is an effective technique for treatment of pulp and paper industrial effluent. The influence of electrolysis time, applied charge density, electrolyte pH and supporting electrolyte on electro-coagulation efficiency for the treatment of pulp and paper industrial effluent has been attempted in the present investigation. It has been observed from the present experimental results that the effluent can be effectively treated using electro-coagulation. The maximum color removal efficiencies were recorded as 92% and 84% for mild steel and aluminum electrode respectively. The maximum COD reduction has been recorded as 95% and 89%. Experiments were also carried out coupling electro-coagulation with sequential batch reactor (SBR) to improve the efficiency of biochemical treatment by increasing the biodegradability index through electro-coagulation. The electro-coagulation was modeled using various adsorption isotherms and observed that the Langmuir and Radke–Prausnitz isotherm models predictions match satisfactorily with the experimental observations.

1. Introduction

Pulp and paper industry is one of the major water-intensive chemical process industries. They are significant contributors of pollutant to the environment in the form of black liquor. The effluent from pulp and paper industry contains high organic matter, suspended solids, strong color, Biological Oxygen Demand (BOD) and Chemical Oxygen Demand (COD). The strong blackish color is mainly attributed to the complex compounds derived from polymerization between lignin-degraded products and tannin during various pulping/bleaching operations. Conventionally, the pulp and paper effluent is treated by physical adsorption, chemical oxidation and biochemical methods. The low biodegradability index (less than 0.4) of pulp and paper effluent clearly shows that this kind of effluent cannot be treated effectively through biochemical method. On the other hand, the chemical methods generate considerable amount of sludge which itself needs further treatment. The drawbacks associated with the conventional techniques forced the industries/researchers for effective treatment method for complete degradation of pollutants [1,2].

In recent years, there has been increasing interest in the use of electrochemical techniques such as electro-coagulation, electro-floatation, electro-oxidation, etc., for the treatment of paper industrial effluent. Among these methods, electro-coagulation emerges as one of the promising techniques due to its unique feature such as complete degradation of pollutants, less sludge generation and easy in operation. Electro-coagulation is a complex and interdependent process where the generation of coagulants takes place in situ by dissolving sacrificial anode. Aluminum or mild steel is mostly used as sacrificial electrode. The mechanism of electro-coagulation can be summarized as follows. When a potential is charged through an external power source, the sacrificial electrodes undergo oxidation as given below:For aluminum electrode:

$$Al_s \rightarrow Al^{3+}_{aq} + 3\ e^- \quad (1)$$

For mild steel electrode:

$$Fe_s \rightarrow Fe^{3+}_{aq} + 3\,e^- \quad (2)$$

The gas generated at the cathode helps to float the flocculated particles, i.e.

$$3\ H_2O_l + 3\,e^- \rightarrow \frac{3}{2}H_{2g} + 3\,OH^-_{aq} \quad (3)$$

The ionic species react to form flocks, i.e., $Fe(OH)_2$ and $Al(OH)_3$ as given below,For aluminum anode

$$Al^{3+}_{aq} + 3\ H_2O_l \rightarrow Al(OH)_{3,s} + 3\,H^+_{aq} \quad (4)$$

For mild steel anode

$$Fe^{3+}_{aq} + 2\,OH^- \rightarrow Fe(OH)_{3,s} \quad (5)$$

* Corresponding author. Present address: School of Engineering, Monash University, Sunway Campus, Malaysia. Tel.: +60 3 551 46231/Mobile: 014 6263425.
E-mail address: n.balasubramanian@eng.monash.edu.my (N. Balasubramanian).

1385-8947/$ – see front matter © 2009 Elsevier B.V. All rights reserved.
doi:10.1016/j.cej.2009.01.050

The flock $Al(OH)_3$)/($Fe(OH)_3$ incarcerates the organic molecules present in the solution by precipitation and/or adsorption mechanism. Successful electro-coagulation treatment of various industrial effluents has been reported by earlier researchers [3,4]. Ugurlu et al. [5] reported more than 70% COD and lignin removal from pulp and paper effluent through electro-coagulation. Mahesh et al. [6] experimented the treatment of pulp and paper mill effluent by electro-coagulation and reported an overall COD removal of 91% with complete color removal. Ben Mansour et al. [7] studied the treatment of paper industrial effluent by coagulation followed electro-floatation and reported more than 95% removal of suspended solids. Though there has been good amount of literature available on electrochemical treatment of pulp and paper effluent, the work related to improvement of biodegradability and isotherm modeling of electro-coagulation process is very scarce. The objective of the present study is to treat the pulp and paper effluent through electro-coagulation. The mechanism of electro-coagulation and the effect of individual parameters on the efficiency of electro-coagulation process have been critically examined. Further it is attempted to model the electro-coagulation process using adsorption isotherms. The effect of electro-coagulation on the biodegradability index of the effluent has also been critically examined.

2. Materials and methods

Three types of experiments were carried out in the present investigation: electro-coagulation, sequential batch reactor, integrated process combining electro-coagulation followed by sequential batch reactor. For electro-coagulation, experiments were carried out in a batch electrochemical reactor of 250 ml capacity having aluminum/mild steel was used as anodes and stainless steel as cathode. The active surface area of the electrode was 16 cm^2. The anode–cathode distance was kept constant at 1.5 cm. The electrodes were cleaned with 15% hydrochloric acid followed by distilled water prior to each experiment. The anode was weighed before and after the each experiment to estimate the electrode consumption. All the experiments were carried out under potentiostatic conditions. The samples were collected at regular intervals of time and analyzed for pollutant degradation. The effluent used in this study was collected from nearby pulp and paper industry and its characteristics are shown in Table 1.

For sequential batch reactor experiments, a laboratory scale SBR having capacity of 1000 ml was used in the present investigation. Proper aeration was provided by air pump with sintered sand diffusers at the bottom of reactor. The required activated sludge was collected from the local municipal sewage treatment plant. The sludge was aerated for 1–2 days at room temperature before inoculating the reactors and subjected for culturing with the effluent. For integrated process, the effluent was treated by electro-coagulation and then subjected for SBR treatment. The pollutant degradations were estimated by dichromate method for COD/BOD estimation using standard procedure [8].

Table 1
Characteristics of pulp and paper effluent.

Characteristics	Value
pH	7.8
Color	Black
COD ($mg\,l^{-1}$)	32,000
BOD ($mg\,l^{-1}$)	8225
BOD/COD	0.26
Suspended solids ($mg\,l^{-1}$)	2200
Dissolved solids ($mg\,l^{-1}$)	5800
Total solids ($mg\,l^{-1}$)	8000

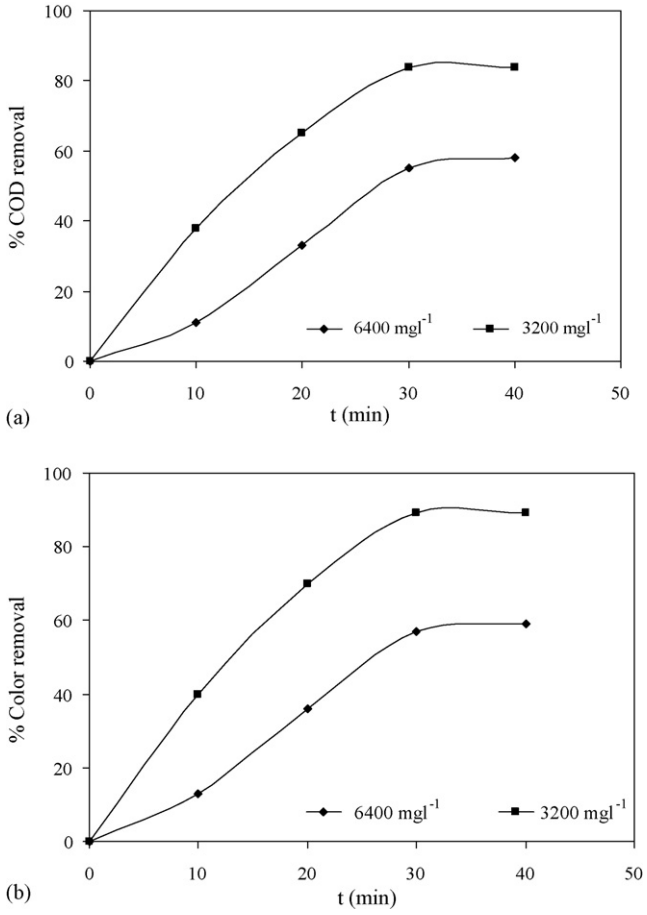

Fig. 1. Variation of (a) percentage COD removal, (b) percentage color removal with electrolysis time; anode: mild steel, pH: 7, current density: 10 $mA\,cm^{-2}$; NaCl: 400 $mg\,l^{-1}$.

3. Results and discussion

Experiments were carried out covering wide range in operating conditions and the observations are presented in the form of tables and figures. Fig. 1a shows the variation of percentage COD removal with process time. It can be noticed from the figure that the percentage COD removal increases with electrolysis time. This is obvious that the $Fe(OH)_3$ flocks are generated in situ once the charge is applied and the generated flocks adsorb the organic molecules present in the effluent resulting reduction in percentage COD with electrolysis time. Notice that more than 50% of COD has been reduced within 15 min of electrolysis. It can be further ascertained that the percentage COD removal decreased with increase in the initial effluent concentration. The percentage COD removal decreased from 91% to 53% when the initial effluent concentration was increased from 3200 $mg\,l^{-1}$ to 6400 $mg\,l^{-1}$. This can be explained that the ratio of hydroxo cationic complexes to the initial effluent concentration decreased with influent concentration. The COD removal is more in the case of mild steel anode than the aluminum anode for the same operating conditions. Similar observations have been recorded for the percentage color removal (Fig. 1b).

3.1. Effect of initial pH

In electro-coagulation, the electrolyte pH plays an important role on the performance of the process [9]. Experiments were carried out at various pH in order to verify the effect of electrolyte

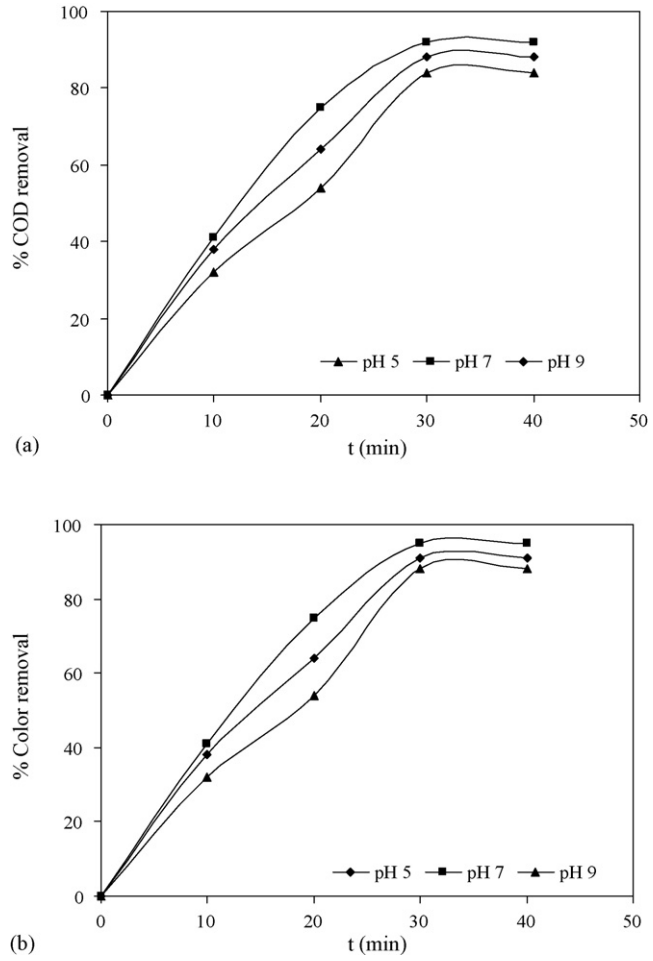

Fig. 2. The effect of electrolyte pH on (a) percentage COD removal, (b) percentage color with electrolysis time; anode: mild steel, current density: 10 mA cm^{-2}; NaCl: 400 mg l^{-1}; influent concentration: 3200 mg l^{-1}.

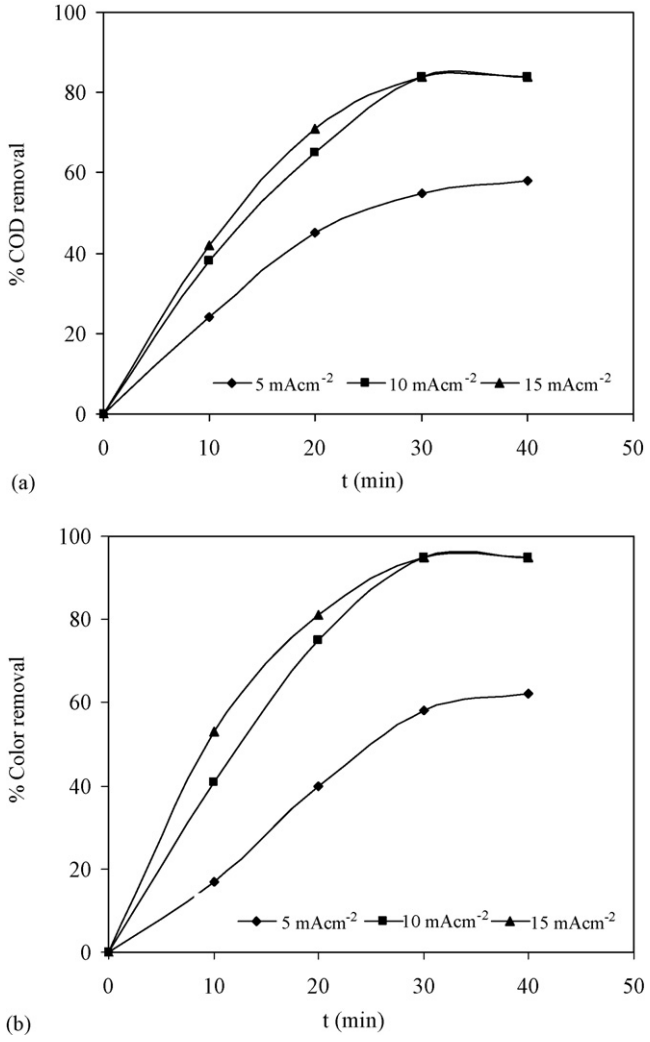

Fig. 3. The influence of applied current density (a) percentage COD removal, (b) percentage color with electrolysis time, anode: aluminum; pH: 5, NaCl: 400 ppm; influent concentration: 3200 mg l^{-1}.

pH on the electro-coagulation efficiency and the observations are given in Fig. 2. The maximum percentage COD removal has been observed at the electrolyte pH of 7 for mild steel electrode (Fig. 2a). Further increase in the electrolyte pH beyond 7 did not yield any improvement on percentage COD removal.

This can be explained that the solubility of $Fe(OH)_3$ increases beyond the electrolyte the pH value of 7 resulting formation of soluble $Fe(OH)_4^-$ which does not contribute to the COD reduction [10]. Similar observation has been recorded for percentage color removal (Fig. 2b).

3.2. Effect of applied current density

It has already been reported by several authors [6,11] that the applied current density has significant influence on the efficiency of the electro-coagulation process. Experiments were carried out by varying applied current density and the observations are given in Fig. 3. It can be ascertained from Fig. 3a that the percentage COD removal increased significantly when the current density increased from 5 mA cm^{-2} to 10 mA cm^{-2}. This can be attributed due to the fact that at high current densities, the extent of anodic dissolution increases and in turn the amount of hydroxo cationic complexes resulting increased COD removal. Further, the applied current density determines the rates of coagulant (flocks formation) and bubble production, which in turn can influence the process efficiency. An increase in the gas bubbles density with reduction in their size enhances upwards flux resulting increased pollutant degradation and sludge floatation [10]. However it can be noticed that increasing the current density beyond 10 mA cm^{-2} did not show any significant improvement in the percentage COD removal.

3.3. Supporting electrolyte concentration

The effect of supporting electrolyte concentration on COD removal efficiency is given in Fig. 4. It can be ascertained from Fig. 4a that the COD removal efficiency increases with an increase in the supporting electrolyte concentration. This can be explained that when chlorides are present in the solution, the products of anodic discharge are Cl_2 and OCl^-. The OCl^- itself a strong oxidant and capable of oxidizing the organic molecules present in the effluent. Thus, the supporting electrolyte not only increases the conductivity but also contributes as strong oxidizing agents. A similar observation has been recorded for the percentage color removal (Fig. 4b).

In electro-coagulation process, the percentage COD removal is proportional to the pollutant concentration and the amount of hydroxides [flocks] generated. The rate equation can be written as

For aluminum:

$$\frac{-\mathrm{d[COD]}}{\mathrm{d}t} = k[\mathrm{COD}][\mathrm{Al(OH)_3}] \quad (6)$$

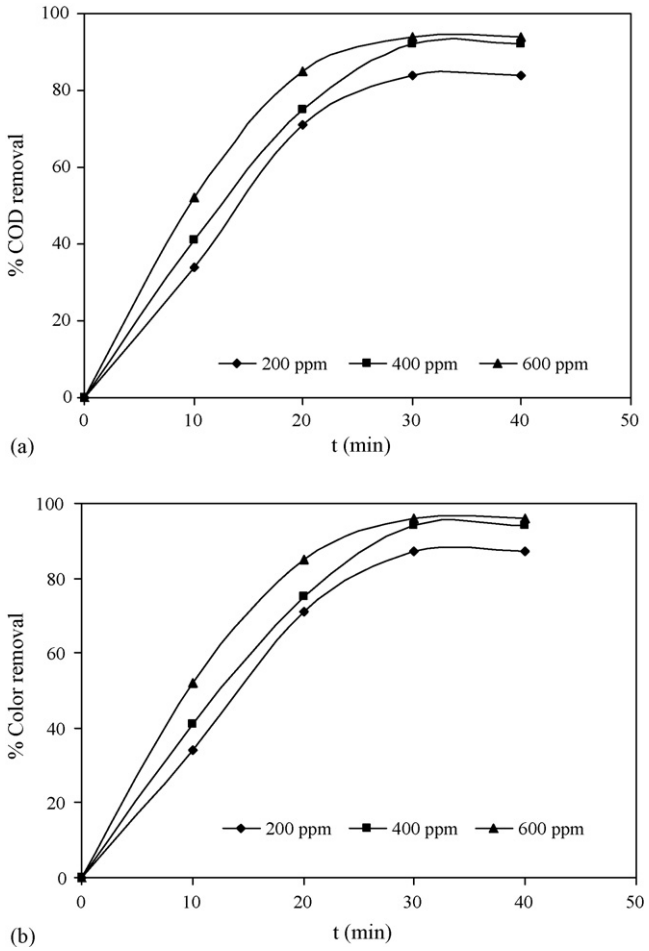

Fig. 4. The effect of supporting electrolyte concentration on (a) percentage COD removal, (b) percentage color with electrolysis time, anode: aluminum, pH: 5, current density: 10 mA cm^{-2}.

For mild steel:

$$\frac{-\mathrm{d[COD]}}{\mathrm{d}t} = k[\mathrm{COD}][\mathrm{Fe(OH)_3}] \quad (7)$$

The above equations can be simplified by assuming the generation of aluminum/ferric hydroxide constant for a given current density as,

$$\frac{-\mathrm{d[COD]}}{\mathrm{d}t} = k[\mathrm{COD}] \quad (8)$$

The integration of Eq. (8) yields

$$\log \frac{[\mathrm{COD}_t]}{[\mathrm{COD}_0]} = -kt \quad (9)$$

where COD_0 refers the initial effluent COD and COD_t refers the effluent COD at time t. The reaction rate constant k, can be estimated from the plot log $[\mathrm{COD}_t/\mathrm{COD}_0]$ versus electrolysis time. The rate constants were estimated for the present experiments and the influence of individual operating parameters on rate constant has been critically examined. Table 2 shows the influence of individual operating parameters on reaction rate. It can be noticed from Table 2 that the reaction rate constant increased with applied current density from 5 mA cm^{-2} to 10 mA cm^{-2}. It can be explained that the rate of coagulant generation increases with applied current density and in turn the reaction rate constant. However, it can be noticed from the table that no significant improvement on rate constant observed when the current density increased beyond 10 mA cm^{-2}. This is due to the fact that the applied charge beyond 10 mA cm^{-2} is used for increasing the electrolyte temperature than the coagulant generation. It can be ascertained from Table 2 that the reaction rate constant is maximum at pH 7 for mild steel electrode, while the maximum reaction rate is observed at pH 5 for aluminum. This is attributed due to fact that the maximum COD removal efficiency has been observed at pH 7 for mild steel (Fig. 2) and pH 5 for aluminum electrode. Finally it can be noticed from Table 2 that the reaction rate constant increases with supporting electrolyte concentration for both aluminum and mild steel electrodes.

3.4. Biodegradability analysis

The biodegradability index (BOD/COD) has been calculated for a typical electro-coagulation process in the present investigation (Fig. 5). It can be ascertained from Fig. 5 that the biodegradability index increased gradually and approaches maximum around 12 min of electro-coagulation. Continuation of electro-coagulation beyond 12 min did not show any significant improvement in the biodegradability index. In fact a small drop in BOD/COD value was observed after 12 min of electro-coagulation. This is due to simultaneous decrease of both COD and BOD beyond 12 min.

Since the BOD/COD value can be increased to beyond 0.4 [which is required for an effective treatment by biochemical technique] within 10 min of electro-coagulation, it was attempted to treat the effluent using sequential batch reactor (SBR) after improving the effluent biodegradability index through electro-coagulation. The effluent was first treated with electro-coagulation for 12 min and then subjected for sequential bath reactor treatment. The SBR experiments were repeated with various combinations of sequences and observed that the sequence of aerobic phase

Table 2
Influence of individual operating parameter on reaction rate constant.

K (min^{-1})/electrode	Parameter			Process conditions
	pH			Initial effluent concentration: 3200 ppm;
	5	7	9	supporting electrolyte concentration:
Al	0.05	0.046	0.046	400 ppm; current density: 10 mA cm^{-2}
MS	0.058	0.07	0.061	
	CD (mA cm^{-2})			Initial effluent concentration: 3200 ppm;
	5	10	15	supporting electrolyte concentration:
Al	0.021	0.051	0.051	400 ppm; electrolyte pH:7
MS	0.023	0.073	0.073	
	NaCl (ppm)			Initial effluent concentration: 3200 ppm;
	200	400	600	electrolyte pH:7; current density: 10 mA cm^{-2}
Al	0.038	0.055	0.058	
MS	0.057	0.071	0.082	

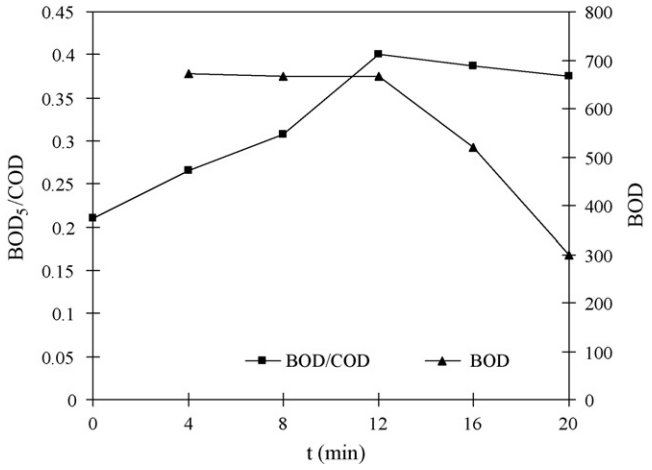

Fig. 5. Effect of electro-coagulation on biodegradability; anode: mild steel, pH: 7; current density: 10 mA cm^{-2}; NaCl: 400 mg l^{-1}.

followed anoxic phase resulted better performance (Fig. 6). It can be seen from Fig. 6 that a maximum percentage removal of 98% has been achieved within 10 h of treatment. The percentage COD removal for the effluent treated directly by SBR (without pre treatment by electro-coagulation) is also given in Fig. 6 for the performance comparison purpose. It can be ascertained from Fig. 6 that the percentage COD removal is only 35% in direct biochemical route during 8 h of operation compared to 90% in integrated process. This clearly indicates that the improvement of biodegradability through electro-coagulation increases the efficiency of SBR very significantly. The percentage COD removal is very marginal in the beginning of aerobic phase due to the acclimation of microorganisms to the system and significant percentage COD removal after 2 h of process time. It can be noticed from Fig. 6 that more than 80% COD removal has been obtained using the aeration phase. The aerobic organisms are activated during aeration which enhances the oxygen based metabolism takes place. It can be noticed that more than 90% COD removal has been obtained at the end of anoxic phase. Fig. 7 shows the effect of pH on percentage COD on SBR process efficiency and observed that the maximum percentage COD removal has been recorded at a pH of 7. This can be explained that the optimum bacterial growth at neutral pH.

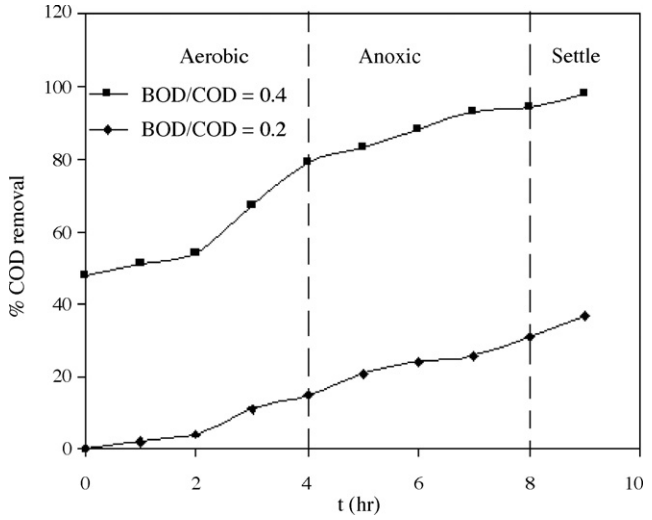

Fig. 6. Treatment of pulp and paper effluent using sequential batch reactor.

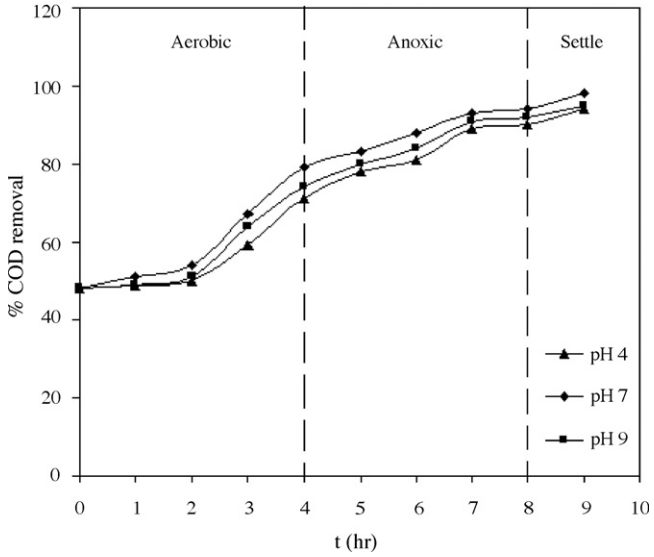

Fig. 7. Effect of pH on COD removal in sequential batch reactor.

4. Adsorption isotherm

The pollutant is generally adsorbed at the surface of the flocks generated during electro-coagulation. Critical analysis of the electro-coagulation of organic pollutants reveals that there are two separate processes, i.e.

- Electrochemical process though which the metal flocks are generated and
- Physio-chemical process through which the effluents are adsorbed on the surface of the flocks.

Thus the removal of pollutant is similar to conventional adsorption except the generation of coagulants. The electrode consumption can be estimated according to Faraday's Law and the amount of flocks generated can be estimated stochiometrically [12]. Since the amount of coagulant can be estimated for a given time, the pollutant removal can be modeled by adsorption phenomenon. It is attempted to test the various adsorption isotherm models for COD removal.

4.1. Two parameter models

4.1.1. Langmuir isotherm

The Langmuir isotherm assumes monolayer deposition of adsorbate on homogenous adsorbent surface (coagulant). It is well known that the Langmuir equation is intended for a homogeneous surface. The mathematical expression of Langmuir isotherm can be given as

$$q_e = \frac{K_L C_e}{1 + a_L C_e} \tag{10}$$

The linearization of Eq. (10) is given as

$$\frac{C_e}{q_e} = \frac{1}{K_L} + \frac{a_L}{K_L} C_e \tag{11}$$

The binding constant (K_L) and the sorbent capacity (a_L) are estimated by plotting C_e/q_e against C_e. The estimated K_L and a_L along with the linear regression coefficient R^2 are given in row R1 of Tables 3 and 4 for mild steel and aluminum electrodes respectively. It can be ascertained from Tables 3 and 4 that the value of K_L increases with an increase in the applied current density. The

Table 3
Estimated two parameter isotherm model parameters for mild steel electrode.

S. no.	Two parameter models	pH (CD:10)			CD (pH: 7)	
		5	7	9	5	15
	Langmuir					
	K_L	0.661	1.565	1.325	0.277	1.8311
R1	a_L	0.00829	0.00377	0.00689	0.00915	0.00086
	R^2	0.996	0.998	0.997	0.968	0.9999
	RMSE	1.58	4.57	1.25	2.47	1.28
	Freundlich					
	K_F	6.574	9.544	8.047	5.219	14.94
R2	n	3.146	7.633	6.083	2.346	11.098
	R^2	0.9254	0.9447	0.9329	0.903	0.9563
	RMSE	10.58	4.78	7.45	8.48	12.89
	Dubinin–Radushkevich					
	q_D	172.604	189.24	173.469	143.825	238.961
R3	b_D	0.0031	0.0056	0.0044	0.0054	0.0863
	R^2	0.8594	0.8905	0.8691	0.8497	0.9115
	RMSE	13.12	14.15	11.25	12.15	11.28

maximum K_L values were recorded at neutral pH for mild steel and at acidic pH for aluminum electrode. The higher value of K_L indicates a high affinity of pollutant towards the flocks. In general high K_L and low a_L values indicate good adsorption characteristic. The higher regression coefficient R^2 substantiates the model fitness with the experimental observation.

4.1.2. Freundlich isotherm

The Freundlich isotherm is an empirical model relates the adsorption intensity of the sorbent towards adsorbent. The isotherm is adopted to describe reversible adsorption and not restricted to monolayer formation. The mathematical expression of the Freundlich model is

$$q_e = K_F C_e^{b_F} \tag{12}$$

where K_F and b_F are the constants which give adsorption capacity and adsorption intensity respectively. A linear form of the Freundlich model can be written as follows

$$\ln\ q_e = \ln K_F + b_F \ln\ C_e \tag{13}$$

A plot of $\ln q_e$ versus $\ln C_e$ gives a straight line with slope K_F and intercept b_F. The values of K_F and b_F along with the linear regression coefficient R^2 for the present experimental conditions have been obtained and are listed in row R2 of Tables 3 and 4 for mild steel and aluminum electrodes respectively. The lower regression coefficients of Freundlich isotherm indicate that the Freundlich isotherm model predictions do not match satisfactorily with the experimental observation.

4.1.3. Dubinin–Radushkevich isotherm

The Dubinin–Radushkevich isotherm model estimates the characteristic porosity of adsorbent and the apparent energy of adsorption. The linear form of Dubinin – Radushkevich isotherm can be given as

$$\ln\ q = \ln\ q_D - B_D\,\varepsilon_D^2 \tag{14}$$

where B_D is related to the free energy of sorption per mole of the sorbate as it migrates to the surface of the coagulant from the solution and q_D is the Dubinin–Radushkevich isotherm constant related to the degree of sorbate sorption by the sorbent surface. The Dubinin–Radushkevich constants are given in row R3 of Tables 3 and 4 for mild steel and aluminum electrodes respectively. It can be seen from the tables that the low regression coefficient of 0.941 for Dubinin–Radushkevich isotherm model indicates that the model predictions do not match with the experimental observation.

4.2. Three parameter models

4.2.1. Redlich–Peterson isotherm

Redlich and Peterson proposed "three parameter" model to represent adsorption equilibrium. The linearization of the expression

Table 4
Estimated two parameter isotherm model parameters for aluminum electrode.

S. no.	Two parameter models	pH (CD:10)			CD (pH: 5)	
		5	7	9	5	15
	Langmuir					
	K_L	0.6644	0.5896	0.4678	0.271	1.0678
R1	a_L	0.001012	0.00228	0.00398	0.006193	0.00051
	R^2	0.996	0.987	0.975	0.8961	0.9996
	RMSE	3.26	2.15	1.58	4.78	1.48
	Freundlich					
	K_F	7.425	4.163	3.26.8	2.572	10.768
R2	n	6.0168	4.1152	3.096	1.863	9.9800
	R^2	0.9657	0.9469	0.8774	0.8861	0.9583
	RMSE	13.72	12.78	14.15	11.89	5.45
	Dubinin–Radushkevich					
	q_D	161.871	158.808	148.205	125.261	239.770
R3	b_D	0.0128	0.0127	0.0116	0.00206	0.1164
	R^2	0.9033	0.8622	0.8319	0.8045	0.9416
	RMSE	13.12	4.18	15.24	14.72	13.85

Table 5
Estimated three parameter isotherm model parameters for mild steel electrode.

S. no.	Three parameter models	pH (CD:10)			CD (pH: 7)	
		5	7	9	5	15
R1	Redlich–Peterson					
	K_{RP}	2	2.863	2.744	1.0	3.21
	a_{RP}	0.045	0.0182	0.024	0.1508	0.0139
	β_{RP}	0.942	0.966	0.962	0.6913	0.9719
	R^2	0.9065	0.946	0.9004	0.9103	0.955
	RMSE	7.661	9.192	5.869	8.846	5.462
R2	Radke–Prausnitz					
	a_R	1.5455	1.983	1.974	1.4322	2.048
	r_R	65.94	140.1	89.46	60.03	150.43
	β_R	0.938	0.965	0.954	0.937	0.976
	R^2	0.9378	0.989	0.9426	0.958	0.999
	RMSE	2.78	3.94	3.299	4.14	5.461
R3	Sips					
	K_S	0.62	0.6501	0.6313	0.6015	0.6721
	a_S	0.1093	0.2637	0.2421	0.1218	0.2799
	β_S	0.968	0.984	0.974	0.968	0.989
	R^2	0.9275	0.940	0.9385	0.9096	0.975
	RMSE	6.241	3.953	4.559	2.54	3.635

gives

$$\ln\left[\frac{K_{RP}C_e}{q_e} - 1\right] = \beta_{RP}\ \ln\ C_e + \ln\ a_{RP} \tag{15}$$

The equation reduces to a linear isotherm at low surface coverage, to the Freundlich isotherm at high adsorbate concentration, and to the Langmuir isotherm when $\beta = 1$. The isotherm constants have been estimated from the plot $\ln[k_{RP}C_e/q_e - 1]$ versus $\ln C_f$. The estimated isotherm constants along the regression coefficient R^2 are listed in row R1 of Tables 5 and 6 for mild steel and aluminum electrodes respectively. The values of isotherm constant K_{RP} and exponent β_{RP} have been observed maximum at neutral pH for mild steel electrode and at pH 5 for aluminum electrode. On the contrary a reverse trend has been observed for a_{RP}. The lower regression coefficient R^2 of Redlich and Peterson isotherm shows that isotherm model does not reflect the present experimental observations.

4.2.2. Radke–Prausnitz isotherm

Radke and Prausnitz suggested an empirical correlation to describe equilibrium for the adsorption of pollutant present in the aqueous solutions on to sorbent. The linear form of Radke–Prausnitz isotherm can be written as

$$\frac{1}{q} = \frac{1}{a_R C_f} + \frac{1}{r_R C_f^{\beta_R}} \tag{16}$$

The Radke–Prausnitz model constants a_R, r_R, and the Radke–Prausnitz model exponent β_R can be estimated by plotting $1/q$ versus $1/C_f$. The estimated Radke–Prausnitz model constants a_R and r_R, the exponent β_R along with the regression coefficient R^2 are listed in row R2 of Tables 5 and 6 for mild steel and aluminum electrodes respectively. The higher value of regression coefficient R^2 indicates that the Radke–Prausnitz predictions match satisfactorily with the experimental observations.

4.2.3. Sips isotherm

Sips isotherms is a combination of the Langmuir and Freundlich isotherms and expected to describe surface heterogeneity. At low sorbate concentrations it reduces to a Freundlich isotherm, while at high sorbate concentrations it predicts a monolayer adsorption capacity characteristic of the Langmuir isotherm. The mathematical

Table 6
Estimated three parameter isotherm model parameters for aluminum electrode.

S. no.	Three parameter models	pH (CD:10)			CD (pH: 5)	
		5	7	9	5	15
R1	Redlich–Peterson					
	K_{RP}	8.26	8.12	7.81	4.87	8.31
	a_{RP}	0.3842	0.5695	0.6816	0.784	0.2911
	β_{RP}	0.9726	0.970	0.968	0.964	0.9823
	R^2	0.9579	0.9359	0.8798	0.8845	0.961
	RMSE	8.005	7.216	10.93	5.086	6.047
R2	Radke–Prausnitz					
	a_R	1.082	0.958.4	0.8146	0.7911	1.850
	r_R	48.12	46.48	45.17	44.18	49.56
	β_R	0.987	0.964	0.960	0.958	0.998
	R^2	0.989	0.978	0.9369	0.9264	0.9975
	RMSE	3.987	5.836	4.726	2.144	5.763
R3	Sips					
	K_S	0.5296	0.4884	0.4549	0.4401	0.5344
	a_S	0.096	0.088	0.076	0.065	0.148
	β_S	0.9781	0.9684	0.9483	0.9324	0.9817
	R^2	0.9671	0.9343	0.8814	0.9285	0.9718
	RMSE	3.925	5.957	4.939	1.679	5.003

expression of Sips isotherm can be written as

$$q_e = \frac{K_s C_e^{\beta_s}}{1 + a_s C_e^{\beta_s}} \quad (17)$$

where K_S is the Sips model isotherm constant (l/g); a_S is the Sips model constant (l/mg) and β_S is the Sips model exponent. A plot of q_e versus C_e enables to determine the constants. Both Sips isotherm parameters and the regression coefficients have been estimated and listed in row R3 of Tables 5 and 6. It can be noticed that the constant K_S is maximum at pH 7 for mild steel electrode and pH 5 for aluminum electrode. The lower value of regression coefficient confirms the Sips isotherm model predictions do not match with the experimental observations.

5. Conclusion

Experiments were carried out to treat pulp and paper effluent using electro-coagulation. The influence of initial effluent concentration, current density, pH and supporting electrolyte concentration on coagulation efficiency using mild steel and aluminum electrodes has been critically examined. The following conclusions have been made based on the present investigation:

(1) The percentage of COD and color reduction was significantly influenced by the initial effluent concentration, pH, supporting electrolyte concentration and current density.
(2) The electro-coagulation was modeled using adsorption isotherm and it has been observed from the present investigation that Langmuir and Radke–Prausnitz isotherm models match satisfactorily with the experimental observations.
(3) The biodegradability of pulp and paper increased through electrocoagulation to more than 0.4 from the original value of 0.2 within 10 min of process time.
(4) The performance of biochemical treatment of pulp and paper effluent has been increased significantly when electrocoagulation is combined with the sequential biological reactor.

References

[1] G. Thompson, J. Swain, M. Kay, C.F. Forster, The treatment of pulp and paper mill effluent: a review, Bioresour. Technol. 77 (2001) 275–286.
[2] T. Kreetachat, M. Damrongsri, V. Punsuwon, P. Vaithanomsat, C. Chiemchaisri, C. Chomsurin, Effects of ozonation process on lignin-derived compounds in pulp and paper mill effluents, Biochem. Eng. J. 35 (2006) 365–370.
[3] G. Chen, X. Chen, P.L. Yue, Electrocoagulation and electroflotation of restaurant waste water, ASCE J. 126 (2000) 858.
[4] H. Inan, A. Dimoglo, H. Simsek, M. Karpuzcu, Olive mill waste water treatment by means of electrocoagulation, Sep. Purif. Technol. 36 (2004) 23–29.
[5] M. Ugurlu, A. Gurses, C. Dogar, M. Yalcin, The removal of lignin and phenol from paper mill effluents by electrocoagulation, J. Environ. Manage. 22 (2007) 52–61.
[6] S. Mahesh, B. Prasad, I.D. Mall, I.M. Mishra, Electrochemical degradation of pulp and paper mill waste water. Part 1. COD and color removal, Ind. Eng. Chem. Res. 45 (2006) 2830–2839.
[7] L. Ben Mansour, I. Ksentini, B. Elleuch, Treatment of wastewaters of paper industry by coagulation–electroflotation, Desalination 208 (2007) 34–41.
[8] APHA, Standard Methods for Examination of Water and Wastewater, 17th ed., American Public Health Association, Washington, DC, 1989.
[9] X. Chen, G. Chen, P.L. Yue, Electrocoagulation and electroflotation of restaurant wastewater, J. Environ. Eng. 126 (9) (2000) 858–863.
[10] M. Kobya, O.T. Can, M. Bayramoglu, Treatment of textile wastewaters by electrocoagulation using iron and aluminum electrodes, J. Hazard. Mater. B100 (2003) 163–178.
[11] N. Adhoum, L. Monser, N. Bellakhal, J.E. Belgaied, Treatment of electroplating wastewater containing Cu^{2+}, Zn^{2+} and Cr(VI) by electro-coagulation, J. Hazard. Mater. B112 (2004) 207–213.
[12] N.K. Khosla, S. Venkachalam, P. Sonrasundaram, Pulsed electrogeneration of bubbles for electroflotation, J. Appl. Electrochem. 21 (1991) 986–990.